

Ho-Meoyng Choi · Chueng-Ryong Ji

Twist-3 Distribution Amplitudes of Pion in the Light-Front Quark Model

Received: date / Accepted: date

Abstract We analyzed two twist-3 distribution amplitudes of pion, i.e. pseudoscalar $\phi_{3;\pi}^P(x)$ and pseudotensor $\phi_{3;\pi}^\sigma(x)$, within the LFQM. Our LFQM descriptions both for twist-3 $\phi_{3;\pi}^P$ and $\phi_{3;\pi}^\sigma$ obtained from the Gaussian radial wave function not only satisfy the fundamental constraint required from the isospin symmetry, but also reproduce exactly the asymptotic forms anticipated from QCD's conformal limit.

Keywords Distribution amplitude · Light-front quark model · Chiral symmetry

1 Introduction

Hadronic light-cone distribution amplitudes (DAs) have been known to play an essential role in the QCD description of hard exclusive processes via the factorization theorem [1]. Taking the transverse separation to zero, the factorization takes the form of a convolution of a perturbatively calculable hard-scattering amplitude and the process-independent nonperturbative DAs. These nonperturbative DAs motivated many theoretical studies to calculate meson DAs using nonperturbative methods such as the QCD sum rule [2; 3; 4], the chiral-quark model from the instanton vacuum [5; 6], the Dyson-Schwinger equations (DSE) approach [7; 8], and the light-front quark model (LFQM) [9; 10; 11; 12]. Among them, the LFQM appears to be one of the most efficient and effective tools in studying hadron physics as it takes advantage of the distinguished features of the light-front dynamics (LFD) [13]. Specifically, the rational energy-momentum dispersion relation of LFD, namely $p^- = (\mathbf{p}_\perp^2 + m^2)/p^+$, yields the sign correlation between the LF energy $p^- (= p^0 - p^3)$ and the LF longitudinal momentum $p^+ (= p^0 + p^3)$ and leads to the suppression of vacuum fluctuations in LFD. This simplification is a remarkable advantage in LFD and facilitates the partonic interpretation of the amplitudes. Based on the advantage of LFD, the LFQM has been quite successful in describing various static and non-static properties of hadrons such as meson mass spectra [14], the decay constants [15], electromagnetic and weak transition form factors [16] and generalized parton distribution (GPDs) [17].

In Ref. [9], we have analyzed twist-2 DAs of pseudoscalar ($\phi_{2;M}^A(x)$) and vector ($\phi_{2;V}^\parallel(x)$) mesons using the LFQM [14]. In more recent works [10; 11], we have extended our LFQM to analyze twist-3 pseudoscalar ($\phi_{3;M}^P(x)$) DAs of pseudoscalar mesons [11] and chirality-even twist-3 ($\phi_{3;V}^\perp(x)$) DAs of

This work was supported by the Korean Research Foundation Grant funded by the Korean Government (No. NRF-2014R1A1A2057457).

H.-M. Choi
Department of Physics, Teachers College, Kyungpook National University, Daegu, Korea 41566
E-mail: homyoung@knu.ac.kr

C.-R. Ji
Department of Physics, North Carolina State University, Raleigh, NC 27695-8202
E-mail: crji@ncsu.edu

vector mesons [10] and discussed the link between the chiral symmetry of QCD and the numerical results of the LFQM. In particular, we have discussed a wave function dependence of the LF zero-mode [18; 19; 20] contributions to $\phi_{3;M}^P(x)$ and $\phi_{3;V}^\perp(x)$ not only for the exactly solvable manifestly covariant Bethe-Salpeter (BS) model but also for the more phenomenologically accessible realistic LFQM [9; 14] using the standard LF (SLF) approach. We also linked the covariant BS model to the standard LFQM providing the correspondence relation [10; 11] between the two models. Effectively, we prescribed a consistent substitution for the LF vertex function in the covariant BS model with the more phenomenologically accessible Gaussian wave function provided by the LFQM analysis of meson mass [14]. The remarkable finding is that the zero-mode contribution as well as the instantaneous contribution revealed in the covariant BS model become absent in the LFQM. Without involving the zero-mode and instantaneous contributions, our LFQM result of twist-3 DAs $\phi_{3;M}^P(x)$ and $\phi_{3;V}^\perp(x)$ provides the consistency with the chiral symmetry anticipated from QCD's conformal limit [2; 21].

The purpose of this work is to extend our previous work [11] to analyze the twist-3 pseudotensor DA $\phi_{3;\pi}^\sigma(x)$ of a pion within the LFQM. The paper is organized as follows: In Sec. 2, we compute the twist-3 pseudotensor DA $\phi_{3;\pi}^\sigma(x)$ in an exactly solvable model based on the covariant BS model of (3+1)-dimensional fermion field theory. We then linked the covariant BS model to the standard LFQM following the correspondence relation [11] between the covariant BS and LFQM models and present the form of $\phi_{3;\pi}^\sigma(x)$ as well as $\phi_{3;\pi}^P(x)$ in our LFQM. In Sec. 3, we present our numerical results. Summary and discussion follow in Sec. 4.

2 Model Description

The $\phi_{3;M}^P$ and $\phi_{3;M}^\sigma$ are defined in terms of the following matrix elements of gauge invariant nonlocal operators in the light-cone gauge [2; 3]:

$$\phi_{3;M}^P(x) = \frac{2(P \cdot \eta)}{f_M \mu_M} \int_{-\infty}^{\infty} \frac{d\tau}{2\pi} e^{-i\zeta\tau(P \cdot \eta)} \langle 0 | \bar{q}(\tau\eta) i\gamma_5 q(-\tau\eta) | M(P) \rangle, \quad (1)$$

$$\phi_{3;M}^\sigma(x) = -\frac{12}{f_M \mu_M} \int_{-\infty}^{\infty} \frac{d\tau}{2\pi} \int_0^x dx' e^{-i\zeta'\tau(P \cdot \eta)} \langle 0 | \bar{q}(\tau\eta) i(\not{P}\not{\eta} - P \cdot \eta) \gamma_5 q(-\tau\eta) | M(P) \rangle, \quad (2)$$

respectively, where $\eta = (1, 0, 0, -1)$ and P is the four-momentum of the meson ($P^2 = m_M^2$) and x corresponds to the longitudinal momentum fraction carried by the quark and $\zeta = 2x - 1$. The normalization parameter $\mu_M = m_M^2 / (m_q + m_{\bar{q}})$ results from quark condensate. For the pion, $\mu_\pi = -2\langle \bar{q}q \rangle / f_\pi^2$ from the Gell-Mann-Oakes-Renner relation [22]. The nonlocal matrix elements $\mathcal{M}_\alpha \equiv \langle 0 | \bar{q}(\tau\eta) i\Gamma_\alpha q(-\tau\eta) | M(P) \rangle$ for pseudoscalar ($\Gamma_\alpha = \gamma_5$) and pseudotensor ($\Gamma_\alpha = (\not{P}\not{\eta} - P \cdot \eta) \gamma_5$) channels are given by the following momentum integral in two-point function of the manifestly covariant BS model

$$\mathcal{M}_\alpha = N_c \int \frac{d^4 k}{(2\pi)^4} e^{-i\tau k \cdot \eta} e^{-i\tau(k-P) \cdot \eta} \frac{\text{Tr} [i\Gamma_\alpha (\not{p} + m_q) \gamma_5 (-\not{k} + m_{\bar{q}})]}{(p^2 - m_q^2 + i\varepsilon)(k^2 - m_{\bar{q}}^2 + i\varepsilon)} H_0, \quad (3)$$

where N_c denotes the number of colors. The quark propagators of mass m_q and $m_{\bar{q}}$ carry the internal four-momenta $p = P - k$ and k , respectively. In order to regularize the covariant loop, we use the usual multipole ansatz [10; 11] for the $q\bar{q}$ bound-state vertex function $H_0 = H_0(p^2, k^2)$ of a meson: $H_0(p^2, k^2) = g / (p^2 - \Lambda^2 + i\varepsilon)^2$, where g and Λ are constant parameters. After a little manipulation, we obtain for the pion ($m_q = m_{\bar{q}}$)

$$\phi_{3;\pi}^P(x) = \frac{N_c}{f_\pi \mu_\pi} \int \frac{d^2 \mathbf{k}_\perp}{8\pi^3} \frac{\chi(x, \mathbf{k}_\perp)}{(1-x)} M_0^2, \quad (4)$$

$$\phi_{3;\pi}^\sigma(x) = -\frac{6N_c}{f_\pi \mu_\pi} \int \frac{d^2 \mathbf{k}_\perp}{8\pi^3} \int_0^x dx' \frac{(2x' - 1) \chi(x', \mathbf{k}_\perp)}{x'(1-x')(1-x')} (\mathbf{k}_\perp^2 + m_q^2), \quad (5)$$

where $\chi(x, \mathbf{k}_\perp) = \frac{g}{[x(m_M^2 - M_0^2)][x(m_M^2 - M_\Lambda^2)]^2}$ and $M_{0(\Lambda)}^2 = \frac{\mathbf{k}_\perp^2 + m_q^2 (\Lambda^2)}{x} + \frac{\mathbf{k}_\perp^2 + m_{\bar{q}}^2}{(1-x)}$.

In the standard LFQM, the wave function of a ground state pseudoscalar meson as a $q\bar{q}$ bound state is given by $\Psi_{\lambda\bar{\lambda}}(x, \mathbf{k}_\perp) = \Phi_R(x, \mathbf{k}_\perp) \mathcal{R}_{\lambda\bar{\lambda}}(x, \mathbf{k}_\perp)$, where Φ_R is the radial wave function and the spin-orbit wave function $\mathcal{R}_{\lambda\bar{\lambda}}$ with the helicity $\lambda(\bar{\lambda})$ of a quark(antiquark) that is obtained by the

interaction-independent Melosh transformation [23; 24] from the ordinary spin-orbit wave function assigned by the quantum numbers J^{PC} . For the radial wave function Φ_R , we use both the gaussian or harmonic oscillator (HO) wave function Φ_{HO} and the power-law (PL) type wave function Φ_{PL} [25] as follows

$$\Phi_{\text{HO}}(x, \mathbf{k}_\perp) = \frac{4\pi^{3/4}}{\beta^{3/2}} \sqrt{\frac{\partial k_z}{\partial x}} e^{-\mathbf{k}^2/2\beta^2}, \quad \Phi_{\text{PL}}(x, \mathbf{k}_\perp) = \sqrt{\frac{128\pi}{\beta^3}} \sqrt{\frac{\partial k_z}{\partial x}} \frac{1}{(1 + \mathbf{k}^2/\beta^2)^2}, \quad (6)$$

where $\mathbf{k}^2 = \mathbf{k}_\perp^2 + k_z^2$ and $k_z = (x-1/2)M_0 + (m_q^2 - m_{\bar{q}}^2)/2M_0$ and β is the variational parameter fixed by the analysis of meson mass spectra [14]. The normalization of Φ_R is given by $\int \frac{dx d^2\mathbf{k}_\perp}{16\pi^3} |\Phi_R(x, \mathbf{k}_\perp)|^2 = 1$.

In our previous analyses of twist-2 and pseudoscalar twist-3 DAs of a pion [11], we have shown that the SLF results in the standard LFQM is obtained by the replacement of the LF vertex function χ in BS model with our LFQM wave function Φ_R as follows (see Eq. (35) in [11])

$$\sqrt{2N_c} \frac{\chi(x, \mathbf{k}_\perp)}{1-x} \rightarrow \frac{\Phi_R(x, \mathbf{k}_\perp)}{\sqrt{\mathbf{k}_\perp^2 + m_q^2}}. \quad (7)$$

The correspondence in Eq. (7) is valid again in this analysis of a pseudotensor twist-3 DA $\phi_{3;\pi}^\sigma(x)$. We now apply this correspondence to both pseudoscalar DA $\phi_{3;\pi}^P(x)$ in Eq. (4) and pseudotensor DA $\phi_{3;\pi}^\sigma(x)$ in Eq. (5) to obtain them in our LFQM as follows:

$$\phi_{3;\pi}^P(x) = \frac{\sqrt{2N_c}}{f_\pi \mu_\pi} \int \frac{d^2\mathbf{k}_\perp}{16\pi^3} \frac{\Phi_R(x, \mathbf{k}_\perp)}{\sqrt{\mathbf{k}_\perp^2 + m_q^2}} M_0^2, \quad (8)$$

$$\phi_{3;\pi}^\sigma(x) = \frac{6\sqrt{2N_c}}{f_\pi \mu_\pi} \int \frac{d^2\mathbf{k}_\perp}{16\pi^3} \int_0^x dx' \frac{(2x' - 1)}{x'(1-x')} \frac{\Phi_R(x', \mathbf{k}_\perp)}{\sqrt{\mathbf{k}_\perp^2 + m_q^2}} (\mathbf{k}_\perp^2 + m_q^2), \quad (9)$$

respectively.

3 Numerical Results

In the numerical computations, we use $m_q = (0.22, 0.25)$ GeV and $\beta_{q\bar{q}} = (0.3659, 0.3194)$ GeV for the linear (HO) confining potential model parameters for the Gaussian wave function, which were obtained from the calculation of meson mass spectra using the variational principle in our LFQM [9; 14]. For the PL wave function, we use $m_q = 0.25$ GeV and $\beta_{q\bar{q}} = 0.335$ GeV adopted from [25]. We first compute the second transverse moments $\langle \mathbf{k}_\perp^2 \rangle_\pi^{P(\sigma)}$ for both pseudoscalar (P) and pseudotensor (σ) channels, and the results obtained from the linear [HO] parameters are given by $\langle \mathbf{k}_\perp^2 \rangle_\pi^P = (553 \text{ MeV})^2 [(480 \text{ MeV})^2]$ and $\langle \mathbf{k}_\perp^2 \rangle_\pi^\sigma = (481 \text{ MeV})^2 [(394 \text{ MeV})^2]$, respectively.

Fig. 1 shows the two-particle twist-3 pion $\phi_{3;\pi}^P(x)$ (left panel) and $\phi_{3;\pi}^\sigma(x)$ (right panel) obtained from the nonzero constituent quark masses using Gaussian wave functions with HO (solid lines) model parameters and PL wave functions (dashed lines). We also plot our results in the chiral symmetry ($m_{u(d)} \rightarrow 0$) limit for both Gaussian (dotted lines) and PL (dot-dashed lines) wave functions and compare them with the chiral-limit prediction of DSE approach employing the dynamical chiral symmetry breaking-improved kernels [8] (double-dot-dashed line) as well as the asymptotic result $6x(1-x)$ (circled data) for the case $\phi_{3;\pi}^\sigma(x)$. Our results for both $\phi_{3;\pi}^P(x)$ and $\phi_{3;\pi}^\sigma(x)$ are normalized without the momentum cutoff (i.e. $|\mathbf{k}_\perp| \rightarrow \infty$).

For $\phi_{3;\pi}^P(x)$ case, our results with nonzero constituent quark masses show rather convex shapes for both Gaussian and PL wave functions but they show quite different end point behaviors, i.e. the end points are more enhanced for the PL wave function than the Gaussian wave function. The difference between the two wave functions are more drastic in the chiral symmetry limit, where the result of Gaussian wave function reproduces the result $\phi_{3;\pi}^P(x) \rightarrow 1$ anticipated from the QCD's conformal limit [2] but the result of PL wave function shows the concave shape similar to the result of DSE approach [8], in which the following asymptotic form $\phi_{3;\pi}^P(x) \rightarrow 1 + (1/2)C_2^{(1/2)}(2x-1)$ was obtained. While the authors in [8] explained that the difference, i.e. $(1/2)C_2^{(1/2)}(2x-1)$ term in chiral symmetry

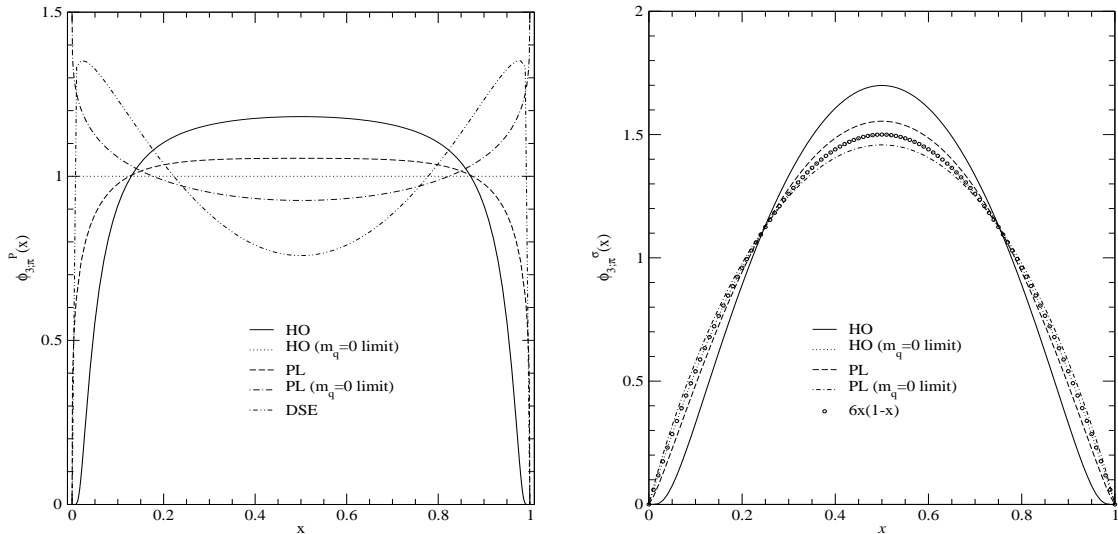


Fig. 1 The twist-3 DAs $\phi_{3;\pi}^P(x)$ (left panel) and $\phi_{3;\pi}^\sigma(x)$ (right panel) of pion.

limit may come from the mixing effect between the two- and three-particle twist-3 amplitudes, we observe that this difference may come from the cutoff scale of the transverse momentum scale associated with the different choice of LF wave functions. Especially, as one can see from Fig. 1, while the end-point suppressed form of $\phi_{3;\pi}^P(x)$ obtained from HO wave function shows constant shape (dotted line) in the chiral symmetry limit, the end-point enhanced form of $\phi_{3;\pi}^P(x)$ obtained from PL wave function shows concave shape (dot-dashed line) in the chiral symmetry limit. The cutoff dependent behaviors of $\phi_{3;\pi}^P(x)$ obtained from both Gaussian and PL wave functions are also presented in [12], where the concave shape for the Gaussian wave function can also be seen with the cutoff scale $\mu = 1$ GeV or less being taken but the cutoff dependence was shown to be more sensitive for the PL wave function than the Gaussian one.

For $\phi_{3;\pi}^\sigma(x)$ case, our results with nonzero constituent quark masses for both Gaussian (solid line) and PL (dashed line) show again different end point behaviors, i.e. the end points are more enhanced for the PL wave function than the Gaussian wave function. However, in the chiral symmetry limit, Gaussian (dotted line) and PL (dot-dashed line) wave functions show very similar shapes each other. Furthermore, the result from Gaussian wave function reproduces exactly the asymptotic form $6x(1-x)$. The same chiral-limit behavior was also obtained from the DSE approach [8]. As one can see from Fig. ??, the twist-3 pseudoscalar $\phi_{3;\pi}^P(x)$ is more sensitive to the shape of the model wave functions (Gaussian vs. PL) than the twist-3 pseudotensor $\phi_{3;\pi}^\sigma(x)$. It is quite interesting to note in the chiral symmetry limit that while $\phi_{3;\pi}^P(x)$ is sensitive to the shapes of model wave functions, $\phi_{3;\pi}^\sigma(x)$ is insensitive to them.

The twist-3 pseudoscalar DA $\phi_{3;M}^P(x)$ and pseudotensor DA $\phi_{3;M}^\sigma(x)$ are usually expanded in terms of the Gegenbauer polynomials $C_n^{1/2}$ and $C_n^{3/2}$, respectively, as follows [6]: $\phi_{3;M}^P = \sum_{n=0}^{\infty} a_{n,M}^P C_n^{1/2}(2x-1)$, and $\phi_{3;M}^\sigma = 6x(1-x) \sum_{n=0}^{\infty} a_{n,M}^\sigma C_n^{3/2}(2x-1)$. The coefficients $a_{n,M}^{P(\sigma)}$ are called the Gegenbauer moments, which describe how much the DAs deviate from the asymptotic one. In addition to the Gegenbauer moments, one can also define the expectation value of the longitudinal momentum, so-called ξ -moments, as follows: $\langle \xi^n \rangle_M^{P(\sigma)} = \int_0^1 dx \xi^n \phi_{3;M}^{P(\sigma)}(x)$. The Gegenbauer- and ξ -moments of the pseudoscalar twist-3 DAs $\phi_{3;\pi}^P(x)$ and twist-2 DA $\phi_{2;\pi}^A(x)$ can be found in our previous works [9; 11].

In Table 1, we list the calculated Gegenbauer- and ξ -moments of pseudotensor twist-3 pion DA $\phi_{3;\pi}^\sigma(x)$ obtained from the Gaussian wave functions with linear and HO potential models and PL wave function. We also compare our results with other model predictions, e.g. QCD sum rules (SR) [3], DSE approach [8] and the chiral quark model (χ QM) [6]. As expected from the isospin symmetry, all odd Gegenbauer and ξ moments are all zero. It is interesting to note that the sign of $a_{2,\pi}^\sigma$ is negative

Table 1 The Gegenbauer moments and ξ moments of twist-3 pion DAs obtained from the linear and HO potential models compared other model estimates.

Models	$a_{2,\pi}^\sigma$	$a_{4,\pi}^\sigma$	$a_{6,\pi}^\sigma$	$\langle \xi^2 \rangle_\pi^\sigma$	$\langle \xi^4 \rangle_\pi^\sigma$	$\langle \xi^6 \rangle_\pi^\sigma$
HO	-0.1155	-0.0268	-0.0046	0.1604	0.0565	0.0263
Linear	-0.0803	-0.0256	-0.0082	0.1725	0.0647	0.0318
PL	-0.0375	-0.0092	-0.0031	0.1871	0.0762	0.0406
SR [3]	0.0979	-0.0016	-0.0011	0.2325	0.1075	0.0624
DSE [8]	0.20	0.085	0.047
χ QM [6]	-0.0984	-0.0192	-0.0037	0.1663	0.0612	-0.0015
$6x(1-x)$	0.20	0.086	0.048

from our LFQM and χ QM predictions but is positive for QCDSR prediction. Larger positive value of $a_{2,\pi}^\sigma$ leads to more flat shape of DA but the larger negative value leads to more narrower shape of DA. Knowing our LFQM results from the HO model are exact to the asymptotic result in the chiral-symmetry limit, i.e. $[\langle \xi^2 \rangle_\pi^\sigma]_{\text{HO}} = [\langle \xi^2 \rangle_\pi^\sigma]_{\text{asy}}$ in $m_q \rightarrow 0$ limit, one can see that the ξ -moments are reduced when the chiral symmetry is broken. We also should note for the same reason that our LFQM results are in good agreement with DSE results in the chiral-symmetry limit of $\phi_{3,\pi}^\sigma(x)$.

4 Summary

We analyzed the two twist-3 DAs of pion, i.e. pseudoscalar $\phi_{3,\pi}^P(x)$ and pseudotensor $\phi_{3,\pi}^\sigma(x)$, within the LFQM. We also investigated the discrepancy of the asymptotic forms of $\phi_{3,\pi}^P(x)$ between DSE approach [8] and QCD's conformal limit expression [2] from the perspective of dependence of DA on the form of LF wave functions, e.g. Gaussian vs. PL wave functions. In order to compute the twist-3 pseudotensor DA $\phi_{3,\pi}^\sigma(x)$, we utilized the same manifestly covariant BS model used in [10; 11; 12] and then substituted the LF vertex function in the covariant BS model with the more phenomenologically accessible Gaussian and PL wave functions. Linking the covariant BS model to the standard LFQM, we used the same correspondence relation Eq. (7) between the two models as the one found in [11; 10]. The remarkable finding in linking the covariant BS model to the standard LFQM is that the treacherous points such as the zero-mode contributions and the instantaneous ones existed in the covariant BS model become absent in the LFQM with the Gaussian or PL wave function.

Our LFQM descriptions for both twist-3 $\phi_{3,\pi}^P$ and $\phi_{3,\pi}^\sigma$ satisfy the fundamental constraint (i.e. symmetric form with respect to x) anticipated from the isospin symmetry. For the $\phi_{3,\pi}^P(x)$ case, our results with nonzero constituent quark masses show rather convex shapes for both Gaussian and PL wave functions but they show quite different end point behaviors, i.e. the end points are more enhanced for the PL wave function than the Gaussian wave function. The difference between the two wave functions are more drastic in the chiral symmetry limit, where the result of Gaussian wave function reproduces the result $\phi_{3,\pi}^P(x) \rightarrow 1$ anticipated from the QCD's conformal limit [2] but the result of PL wave function shows the concave shape similar to the result of DSE approach [8]. For the $\phi_{3,\pi}^\sigma(x)$ case, our results from both Gaussian and PL wave functions in the chiral symmetry limit, show very similar shapes each other. Especially, the result from Gaussian wave function reproduces exactly the asymptotic form $6x(1-x)$ anticipated from QCD's conformal limit. The same chiral-limit behavior was also obtained from the DSE approach [8]. The remarkable thing is that our predictions for the two twist-3 DAs of π and chirality-even twist-2 DA $\phi_{2,\rho}^\parallel(x)$ and twist-3 DA $\phi_{3,\rho}^\perp(x)$ of ρ [10] obtained from the Gaussian wave function in the chiral limit exactly reproduce the forms anticipated from QCD's conformal limit. We summarize in Table 2 the asymptotic forms for the two twist-3 DAs of π and chirality-even twist-2 and twist-3 DAs of rho meson compared with DSE approach [8] and QCD's conformal limit expression [2; 21].

The idea of our LFQM is to provide the nonperturbative wave functions at the momentum scale consistent with the use of constituent quark mass. The DAs determined from this nonperturbative wave functions can be fed into the QCD evolution equation to provide the shorter distance information of the corresponding hadrons. While our results for both $\phi_{3,\pi}^P$ and $\phi_{3,\pi}^\sigma$ in Fig. 1 were obtained without the momentum cutoffs (i.e. $|\mathbf{k}_\perp| \rightarrow \infty$), the scales of both DAs obtained from the Gaussian wave functions and that of $\phi_{3,\pi}^\sigma$ obtained from PL wave function are estimated to be $|\mathbf{k}_\perp| \simeq 1$ GeV. However, the scale

Table 2 Asymptotic forms of various DAs of π and ρ .

Model in $m_q \rightarrow 0$	$\phi_{3;\pi}^P$	$\phi_{3;\pi}^\sigma$	$\phi_{2;\rho}^\parallel(x)$	$\phi_{3;\rho}^\perp(x)$
LFQM (HO model) [10; 11]	1	$6x(1-x)$	$6x(1-x)$	$\frac{3}{4}[1+(2x-1)^2]$
DSE approach [8]	$1 + \frac{1}{2}C^{1/2}2(2x-1)$	$6x(1-x)$	—	—
QCD's conformal limit [2; 21]	1	$6x(1-x)$	$6x(1-x)$	$\frac{3}{4}[1+(2x-1)^2]$

of $\phi_{3;\pi}^P$ obtained from PL wave function are estimated to $|\mathbf{k}_\perp| \simeq 2$ GeV due to the high momentum tail compared to other wave functions. The DAs obtained without the cutoff should not be regarded as the fully evolved DAs but still be nonperturbative as they just mean that the cutoff dependence becomes marginal beyond a certain nonperturbative cutoff scale.

References

1. Lepage, G.P., Brodsky, S. J: Exclusive Processes in Perturbative Quantum Chromodynamics. Phys. Rev. D **22**, 2157 (1980).
2. Braun, V.M., Filyanov, I.E.: Conformal Invariance and Pion Wave Functions of Nonleading Twist. Z. Phys. C **48**, 239 (1990).
3. Ball, P., Braun, V.M., Lenz, A.: Higher-twist distribution amplitudes of the K meson in QCD. J. High Energy Phys. 05, 004 (2006).
4. Mikhailov, S.V., Pimikov, A.V., Stefanis, N.G.: Endpoint behavior of the pion distribution amplitude in QCD sum rules with nonlocal condensates. Phys. Rev. D **82**, 054020 (2010).
5. Petrov, V.Y., Polyakov, M.V., Ruskov, R., Weiss, C., Goeke, K.: Pion and photon light-cone wave functions from the instanton vacuum. Phys. Rev. D **59**, 114018 (2006).
6. Nam, S.I., Kim, H.-Ch.: Twist-3 pion and kaon distribution amplitudes from the instanton vacuum with flavor SU(3) symmetry breaking. Phys. Rev. D **74**, 096007 (2006).
7. Chang, L., Roberts, C.D., Schmidt, S.M.: Light front distribution of the chiral condensate. Phys. Lett. B **727**, 255 (2013).
8. Shi, C., Chen, C., Chang, L., Roberts, C.D., Schmidt, S.M., Zong, H.-S.: Kaon and pion parton distribution amplitudes to twist three. Phys. Rev. D **92**, 014035 (2015).
9. Choi, H.-M., Ji, C.-R.: Distribution amplitudes and decay constants for (π, K, ρ, K^*) mesons in the light-front quark model. Phys. Rev. D **75**, 034019 (2007).
10. Choi, H.-M., Ji, C.-R.: Self-consistent covariant description of vector meson decay constants and chirality-even quark-antiquark distribution amplitudes up to twist 3 in the light-front quark model. Phys. Rev. D **89**, 033011 (2014).
11. Choi, H.-M., Ji, C.-R.: Consistency of the light-front quark model with chiral symmetry in the pseudoscalar meson analysis. Phys. Rev. D **91**, 014018 (2015).
12. Choi, H.-M., Ji, C.-R.: Light-Front Quark Model Phenomenology Consistent with Chiral Symmetry. EPJ Web of Conference **113**, 05009 (2016).
13. Brodsky, S. J., Pauli, H. -C. , Pinsky, S.: Quantum chromodynamics and other field theories on the light cone. Phys. Rep. **301**, 299 (1998).
14. Choi, H.-M., Ji, C.-R.: Mixing angles and electromagnetic properties of ground state pseudoscalar and vector meson nonets in the light-cone quark model. Phys. Rev. D **59**, 074015 (1999).
15. Choi, H.-M.: Decay constants and radiative decays of heavy mesons in light-front quark model. Phys. Rev. D **75**, 073016 (2007).
16. Choi, H.-M., Ji, C.-R.: Semileptonic and radiative decays of the B(c) meson in light-front quark model. Phys. Rev. D **80**, 054016 (2009).
17. Choi, H.-M., Ji, C.-R., Kisslinger, L.S.: Skewed quark distribution of the pion in the light front quark model. Phys. Rev. D **64**, 093006 (2001).
18. Brodsky, S.J., Hwang, D.S.: Exact light cone wave function representation of matrix elements of electroweak currents. Nucl. Phys. B **543**, 239 (1998).
19. de Melo, J.P.B.C., Sales, J.H.O., Frederico, T., Sauer, P.U.: Pairs in the light front and covariance. Nucl. Phys. A **631**, 574c (1998).
20. Choi, H.-M., Ji, C.-R.: Nonvanishing zero modes in the light front current. Phys. Rev. D **58**, 071901(R) (1998).
21. Ball, P., Braun, V.M., Koike, Y., Tanaka, K.: Higher twist distribution amplitudes of vector mesons in QCD: Formalism and twist - three distributions. Nucl. Phys. B **529**, 323 (1998).
22. Gell-Mann, M., Oakes, R., Renner, B.: Behavior of current divergences under $SU(3) \times SU(3)$. Phys. Rev. **175**, 2195 (1968).
23. Melosh, H.J.: Quarks: Currents and constituents Phys. Rev. D **9**, 1095 (1974);
24. Chung, P.L., Coester, F., Keister, B.D., Polyzou, W.N.: Hamiltonian Light Front Dynamics of Elastic electron Deuteron Scattering. Phys. Rev. D **37**, 2000 (1988).
25. Schlumpf, F.: Charge form factors of pseudoscalar mesons. Phys. Rev. D **50**, 6895 (1994).